Tethered Monolayers of Poly((*N*-pyrrolyl)alkanethiol) on Au†

Robin L. McCarley* and Robert J. Willicut‡

Contribution from the Choppin Laboratories of Chemistry, Louisiana State University, Baton Rouge, Louisiana 70803-1804

Received May 14, 1998

Abstract: The electrochemical oxidation of pyrrole-terminated, self-assembled alkanethiol monolayers on Au surfaces in dry electrolyte media (<0.005% H_2O) results in tethered poly(*N*-alkylpyrroles) of varying monomer repeat lengths. After pristine (monomeric) monolayers of 10-(*N*-pyrrolyl)decane-1-thiol (**1**), 7-(*N*-pyrrolyl)-heptane-1-thiol (**2**), and 6-(*N*-pyrrolyl)hexane-1-thiol (**3**) on Au have been oxidized in nonaqueous electrolyte media, electrochemistry characteristic of poly(*N*-alkylpyrroles) is observed. Reflection−absorption infrared spectra of the oxidized monolayers exhibit aromatic C−H out-of-plane deformation bands between 700 and 800 cm^{-1} that can be used to determine the effective conjugation length of the poly(*N*-alkylpyrroles) produced. The number of monomer repeat units in the backbone ranges from 2 to ∼20 and depends on the oxidation potential applied to the monomeric monolayers. In comparison to the monomeric monolayers, the electrochemically polymerized monolayers are demonstrated to be more stable with respect to exchange by a redox-labeled alkanethiol.

Chemical reactions in and at supported molecular assemblies represent an area of surface chemistry that is becoming prevalent in disciplines ranging from materials science to biology.[1] This popularity is based in part on the demand for surfaces with highly specific characteristics and the wide variety of possible surface functionalities available with monomolecular films.[2] Self-assembled monolayers of alkanethiols on the coinage metals[2,3] are extremely attractive when considering the available options in the field of monomolecular films—much is known about the molecular structure of *n*-alkanethiols on Au and Ag, and ω-functionalized alkanethiol monolayers are, for the most part, readily accessible through well-established synthetic procedures. As a result, self-assembled monolayers of alkanethiols have been widely explored for use in applications such as adhesion promotion, corrosion-resistant coatings, chemical force microscopy, "soft" lithography, small-molecule and biological sensors, and molecular electronics.[1−3]

A topic in the area of chemical reactions in surface-confined monolayers that has been of interest to our group and others is that of polymerizations.[4] The work with monomeric self-assembled monolayers has at its foundation the wealth of information gained from the study of polymerizations in organized media such as Langmuir−Blodgett films and micelles.[5] Surface-immobilized monomers offer the unique opportunity to fully explore the effects of monomer molecular environment on the polymerization process—effects that will be important to the construction of nanometer-sized materials.[6] Variations in the orientation of the monomer groups with respect to the substrate and each other, the concentration of monomer

* Corresponding author: (phone) (225) 388-3239; (facsimile) (225) 388-3458; (e-mail) tunnel@unix1.sncc.lsu.edu.

† This paper is the fifth in a series of contributions from LSU titled *Monomers on Electrode Surfaces*.

‡ Current address: The Procter and Gamble Co., Cincinnati, OH 45241-2422.

(1) (a) Kurth, G. G.; Bein, T. *Langmuir* **1993**, *9*, 2965. (b) Frostman, L.; Bader, M. M.; Ward, M. D. *Langmuir* **1994**, *10*, 576. (c) Keller, S. W.; Kim, H.-N.; Mallouk, T. E. *J. Am. Chem. Soc.* **1994**, *116*, 8817. (d) Tao, Y.-T.; Lin, W. L.; Hietpas, G. D. *J. Phys. Chem. B* **1997**, *101*, 9732. (e) Fox, M. A.; Whitesell, J. K.; McKerrow, A. J. *Langmuir* **1998**, *14*, 816. (f) Dunaway, D. J.; McCarley, R. L. *Langmuir* **1994**, *10*, 3598. (g) Delamarche, E.; Sundarababu, G.; Biebuyck, H.; Michel, B.; Gerber, C.; Sigriat, H.; Wolf, H.; Ringsdorf, H.; Xanthopoulos, N.; Mathieu, H. J. *Langmuir* **1996**, *12*, 1997. (h) Mrksich, M.; Sigal, G. B.; Whitesides, G. M. *Langmuir* **1995**, *11*, 4383. (i) Wagner, P. J.; Hegner, M.; Kernen, P.; Zaugg, F.; Semenza, G. *Biophys. J.* **1996**, *70*, 2052.

(2) (a) Ulman, A. In *An Introduction to Ultra-Thin Films: From Langmuir−Blodgett to Self-Assembly*; Academic: San Diego, CA, 1991. (b) Ulman, A. *Chem. Rev.* **1996**, *96*, 1533.

(3) (a) Whitesides, G. M.; Mathias, J. P.; Seto, C. T. *Science* **1991**, *254*, 1312. (b) Dubois, L. H.; Nuzzo, R. G. *Annu. Rev. Phys. Chem.* **1992**, *43*, 437. (c) Whitesides, G. M. *Sci. Am.* **1995**, *273*, 146. (d) Zhong, C.-J.; Porter, M. D. *Anal. Chem.* **1995**, *67*, 709A. (e) Delamarche, E.; Michel, B.; Biebuyck, H. A.; Gerber, C. *Adv. Mater.* **1996**, *8*, 719.

(4) (a) Willicut, R. J.; McCarley, R. L. *J. Am. Chem. Soc.* **1994**, *116*, 10823. (b) T. Kim, R. M. Crooks, *Tetrahedron Lett.* **1994**, *35*, 9501. (c) Batchelder, D. N.; Evans, S. D.; Freeman, T. L.; Häussling, L.; Ringsdorf, H.; Wolf, H. *J. Am. Chem. Soc.* **1994**, *116*, 1050. (d) Kim, T.; Chan, K. C.; Crooks, R. M. *J. Am. Chem. Soc.* **1997**, *119*, 189. (e) Willicut, R. J.; McCarley, R. L. *Anal. Chim. Acta* **1995**, *307*, 269. (f) Ford, J. F.; Vickers, T. J.; Mann, C. K.; Schlenoff, J. B. *Langmuir* **1996**, *12*, 1944. (g) Hayes, W. A.; Shannon, C. *Langmuir* **1996**, *12*, 3688. (h) Peanasky, J. S.; McCarley, R. L. *Langmuir* **1998**, *14*, 113. (i) Sayre, C. N.; Collard, D. M. *Langmuir* **1995**, *11*, 302. (j) Wurm, D. B.; Zong, K.; Kim, Y.-H.; Kim, Y.-T.; Shin, M.; Jeon, I. C. *J. Electrochem. Soc.* **1998**, *145*, 1483. (k) Smela, E.; Kariis, H.; Yang, Z.; Uvdal, K.; Zuccarello, G.; Liedberg, B. *Langmuir* **1998**, *14*, 2876. (l) Lin, S.; McCarley, R. L. Submitted to *Langmuir*, 1998. (m) Mowery, M. D.; Evans, C. E. *J. Phys. Chem. B* **1997**, *101*, 8513.

(5) (a) Cemel, A.; Fort, T., Jr.; Lando, J. B. *J. Polym. Sci. A-1* **1972**, *10*, 2061. (b) Ackermann, R.; Inacker, O.; Ringsdorf, H. *Kolloid-Z. Z. Polym.* **1971**, *249*, 1118. (c) Barraud, A.; Rosilio, C.; Ruaudel, A. *J. Colloid Interface Sci.* **1977**, *62*, 509. (d) Xu, S. Q.; Fendler, J. H. *Macromolecules* **1989**, *22*, 2962. (e) Bodalia, R.; Manzanares, J.; Reiss, H.; Duran, R. *Macromolecules* **1994**, *27*, 2002. (f) Sagisaka, S.; Ando, M.; Iyoda, T.; Shimidzu, T. *Thin Solid Films* **1993**, *230*, 65. (g) Iyoda, T.; Ando, M.; Kaneko, T.; Ohtani, A.; Shimidzu, T.; Honda, K. *Tetrahedron Lett.* **1986**, *27*, 5633. (h) Rikukawa, M.; Rubner, M. F. *J. Mater. Sci., Pure Appl. Chem.* **1994**, *A31*, 793. (i) Yang, X. Q.; Chen, J.; Hale, P. D.; Inagaki, T.; Skotheim, T. A.; Okamato, Y.; Samuelson, L.; Tripathy, S.; Hong, K.; Rubner, M. F.; denBoer, M. L. *Synth. Met.* **1989**, *28*, C251. (j) Reed, W.; Gutreman, L.; Tundo, P.; Fendler, J. H. *J. Am. Chem. Soc.* **1984**, *106*, 1897. (k) Peek, B. M.; Callhan, J. H.; Namboodiri, K.; Singh, A.; Gaber, B. P. *Macromolecules* **1994**, *27*, 292. (l) Tyminski, P. N.; Ponticello, I. S.; O'Brien, D. F. *J. Am. Chem. Soc.* **1987**, *109*, 6541. (m) Wang, J.; Warner, I. M. *Anal. Chem.* **1994**, *66*, 3773. (n) Dobashi, A.; Hamada, M.; Dobashi, Y. *Anal. Chem.* **1995**, *67*, 3011.

S0002-7863(98)01677-1 CCC: $15.00
Published on Web 08/28/1998

sites within the monolayer,[4e,h,7] and structure of the monolayer as a result of crystallographic orientation[8] or curvature of the metal support[4h,9] should give rise to information on how to manipulate polymerization reactions in self-assembled monolayer films. Not only is this information of importance to the understanding of polymerization reactions at the nanometer scale but it will also assist those focused on the building of complex structures that may be used in sensing, submicron fabrication, and "molecular" electronic components. In particular, we have an interest in being able to electrochemically form nanometer-sized organic conducting polymer features in monomeric monolayer surfaces using electrochemical reactions that can be made to occur near the tip of a scanning probe microscope.[6e,f] In addition, we are intrigued by the possibility that increases in the stability of alkanethiol monolayers with respect to desorption in various media can be achieved by polymerizing the monolayer.[4d] Furthermore, such polymerization of a self-assembled monolayer may also enhance stability with respect to ozone oxidation.[10] The following describes our recent efforts at understanding the structure of a series of *ω*-(*N*-pyrrolyl)-alkanethiols **1**−**5** on Au surfaces before and after electrochemical polymerization of the pyrrole groups and how such polymerization chemistry can be used for the stabilization of self-assembled monolayers.

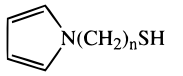

1-5 n = 10, 7, 6, 5, and 3

Results and Discussion

Pristine *ω*-(*N*-Pyrrolyl)alkanethiol Monolayers. The electrochemical response of **1**/Au in 0.1 M Bu_4NClO_4/propylene carbonate is displayed in Figure 1A. The voltammetry is virtually indistinguishable from that observed for monolayers of **2** and **3**[4a] on Au. In addition, identical behavior was observed for **1**−**3** on Au when acetonitrile was used as the electrochemical solvent. Potential excursions to +1.40 V vs Ag QRE (Figure 1A) result in complete and irreversible oxidation of the surface-confined pyrrole groups, as noted by the lack of a cathodic wave during the first scan and the absence of current near the anodic peak oxidation potential $E_{p,ox}$ of ∼+1.15 V vs Ag QRE in subsequent voltammetric scans. It was also observed that $E_{p,ox}$ for the surface-confined pyrroles is virtually independent of the number of methylene spacers between the thiol headgroup and the pyrrole tail. Au electrodes coated with simple *n*-alkanethiol monolayers do not exhibit any voltammetric features in this potential range. As we previously reported for **3**−**5**,[4a] the peak anodic current $i_{p,ox}$ scales linearly with potential scan rate υ over the range of scan rates investigated (0.05−0.50 V s^{-1}), confirming that the voltammetric signal results from the presence of immobilized redox species on the Au electrode.[11,12] These data are in accord with the electrochemical production of surface-confined pyrrole radical cations; such pyrrole radicals can react with each other to produce poly(pyrroles) **7**,[13] or these radicals can be deactivated by nucleophiles such as water to eventually yield products such as those in Scheme 1 **8**−**10** (vide infra).[14−16] In addition, X-ray photoelectron spectra (XPS) of

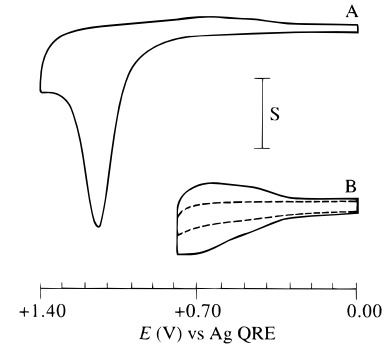

Figure 1. Cyclic voltammograms of **1**/Au in 0.1 M Bu_4NClO_4/propylene carbonate. (A) Initial voltammetric scan of **1**/Au. (B) Voltammetric scan after the potential excursion in A. Conditions for A and B: $\upsilon = 0.10$ V s^{-1}, $S = 19.2 \times 10^{-6}$ A cm^{-2} in A and 7.7×10^{-6} A cm^{-2} in B. The dotted line in B represents the response of the monomeric monolayer before the potential excursion to +1.40 V in A.

Scheme 1

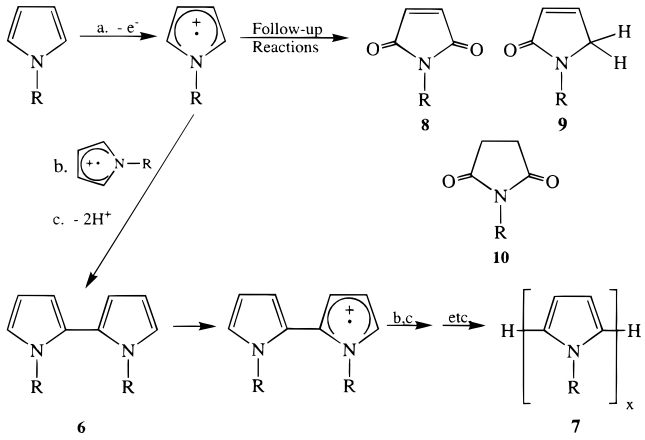

(6) (a) Bard, A. J. *Integrated Chemical Systems: A Chemical Approach to Nanotechnology*; Wiley: New York, 1994. (b) *Proceedings of The Robert A. Welch Foundation, 40th Conference on Chemical Research: Chemistry on the Nanometer Scale*; Welch Foundation: Houston, TX, 1996. (c) Ozin, G. A. *Adv. Mater.* **1992**, *4*, 612. (d) Hostetler, M. J.; Murray, R. W. *Curr. Opin. Colloid Interface Sci.* **1997**, *2*, 42. (e) Penner, R. M. *Scanning Microsc.* **1993**, *7*, 805. (f) McCarley, R. L.; Hendricks, S. A.; Bard, A. J. *J. Phys. Chem.* **1992**, *96*, 10089.

(7) Bain, C. D.; Whitesides, G. M. *Science* **1988**, *240*, 62.

(8) Strong, L.; Whitesides, G. M. *Langmuir* **1988**, *4*, 546.

(9) (a) Brust, M.; Walker, M.; Bethell, D.; Schiffrin, D. J.; Whyman, R. *J. Chem. Soc., Chem. Commun.* **1994**, 801. (b) Terrill, R. H.; Postlewaite, T. A.; Chen, C.-H.; Poon, C.-D.; Terzis, A.; Chen, A.; Hutchinson, J. E.; Clark, M. R.; Wignall, G.; Londono, J. D.; Superfine, R.; Falvo, M.; Johnson, C. S., Jr.; Samulski, E. T.; Murray, R. W. *J. Am. Chem. Soc.* **1995**, *117*, 12537. (c) Badia, A.; Singh, S.; Demers, L.; Cuccia, L.; Brown, G. R.; Lennox, R. B. *Chem. Eur. J.* **1996**, *2*, 359. (d) Whetten, R. L.; Khoury, J. T.; Alvarez, M. M.; Murthy, S.; Vezmar, I.; Wang, Z. L.; Stephens, P. W.; Cleveland, C. L.; Luedtke, W. D.; Landman, U. *Adv. Mater.* **1996**, *8*, 428. (e) Heath, J. R.; Knobler, C. M.; Leff, D. V. *J. Phys. Chem. B* **1997**, *101*, 189.

(10) (a) The oxidation of the sulfur headgroup in *n*-alkanethiol monolayers on Au has been a topic of great interest over the past few years.[10b−f] Only recently has the cause of such oxidation been determined; the presence of ozone in laboratories during monolayer preparation, the amount of which greatly varies depending on the locale, has been shown to be the culprit.[10g] (b) Li, Y.; Huang, J.; McIver, R. T., Jr.; Hemminger, J. C. *J. Am. Chem. Soc.* **1992**, *114*, 2428. (c) Tarlov, M. J.; Newmann, J. G. *Langmuir* **1992**, *8*, 1398. (d) Horn, A. B.; Russell, D. A.; Shorthouse, L. J.; Simpson, T. R. E.; *J. Chem. Soc., Faraday Trans.* **1996**, *92*, 4759. (e) Wilkins, C. L.; Scott, J. R.; Yao, J.; Fritsch, I.; Everett, W. R. In *Proceedings of the 45th ASMS Conference on Mass Spectrometry and Allied Topics*; Portland, OR, May 12−16, 1996; p 1131. (f) Scott, J. R.; Baker, L. S.; Everett, W. R.; Wilkins, C. L.; Fritsch, I. *Anal. Chem.* **1997**, *69*, 2636. (g) Schoenfisch, M. H.; Pemberton, J. E. *J. Am. Chem. Soc.* **1998**, *120*, 4502.

(11) Bard, A. J.; Faulkner, L. J. *Electrochemical Methods: Fundamentals and Applications*; Wiley: New York, 1980.

(12) Moses, P. R.; Murray, R. W. *J. Am. Chem. Soc.* **1976**, *98*, 7435.

(13) Skotheim, T. A., Ed. *Handbook of Conducting Polymers*; Marcel Dekker: New York, 1986.

(14) (a) Smith, E. B.; Jensen, H. B. *J. Org. Chem.* **1967**, *32*, 3330. (b) Bocchi, V.; Chierici, L.; Gardini, G. P.; Mondelli, R. *Tetrahedron* **1970**, *26*, 4073.

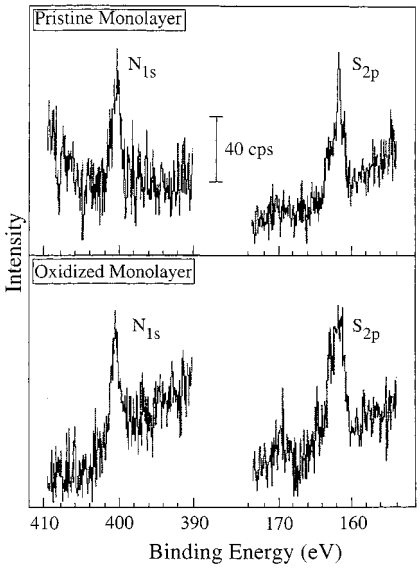

Figure 2. X-ray photoelectron spectra of **1**/Au in the N_{1s} and S_{2p} regions before and after oxidation to $E_{p,ox}$ +0.1 V (+1.25 V vs Ag QRE) and emmersion at $E_{p,ox}$ −1.15 V (0 V vs Ag QRE) in 0.1 M Bu_4NClO_4/propylene carbonate.

the pyrrole monolayers on Au display N_{1s} and S_{2p} signals whose integrated band intensities remain unchanged upon oxidation to +1.40 V vs Ag QRE, Figure 2. These observations indicate that monolayers of **1**−**3** are not oxidatively desorbed[17] under the voltammetric conditions used in Figure 1A. In addition, monolayers of **3** on Au electrodes were only moderately effective mass transport barriers, as noted in voltammetric blocking experiments that employed $[Fe(CN)_6]^{3-}$ as the probe molecule; the peak potential separation was found to be ∼0.5 V, and the peak currents were roughly 65% of those at bare Au. Finally, it is found that the surface density Γ_{ox} (mol cm^{-2}) of pyrrole functionalities obtained by integration of the voltammetric wave[18a] is independent of the number of methylene units between the thiol anchoring group and the pyrrole tail, with a mean value of 3.8×10^{-10} mol cm^{-2} being obtained. This value of surface coverage for the pyrrole monolayer is roughly one-half that of *n*-alkanethiols (7.8×10^{-10} mol cm^{-2}) on similarly prepared Au substrates[17] and indicates that the size of the pyrrole moiety dictates the packing density or "footprint" of the adsorbate. In total, the voltammetric results point to a very open monolayer structure.

Reflection−absorption infrared spectroscopy (RAIRS)[19] experiments carried out on pristine monolayers of **1**−**3** on evaporated Au support an open or "floppy" monolayer structure. The liquid transmission IR spectrum of **1** and RAIR spectrum

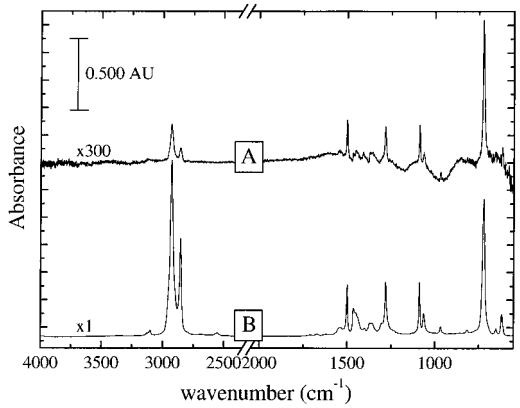

Figure 3. Infrared spectra of **1**. (A) Reflection−absorption spectrum on Au. (B) Liquid transmission spectrum. An octadecane-1-thiol-d_{37}/Au slide was used as the background in A.

of **1**/Au are displayed in Figure 3. Band assignments[20−22] for the observed infrared-active modes of **1** are compiled in Table 1; band positions very similar to those of **1** were observed for **2** and **3**. RAIR spectra of **1**−**3** on Au remained unchanged when emmersed samples were stored in either the drybox or the nitrogen-purged IR chamber for times up to 16 h, indicating that oxidation of the monolayers by oxygen or ozone[10] at the levels present in these environments (∼1 ppm for oxygen, unknown for ozone) is not a concern. From the selection rules of RAIRS, one would expect that if there existed a preferred orientation of **1** on a Au surface, i.e., vibrational modes with their transition dipole moments oriented in a particular fashion, there would be differences in the intensity ratios of a given pair of bands when moving from the isotropic spectrum to the reflection spectrum.[19] On the other hand, if there is no one particular orientation that is favored for the assembled layer, then one would expect small differences in the ratio of intensities of two particular bands when comparing the transmission and RAIR spectra. The latter case is observed for the modes associated with the pyrrole ring when the liquid transmission spectra and the reflection spectra of **1**−**3** are compared. For example in Figure 3, the band intensity ratio of the $\nu(C-N)_{aliphatic}$ and $\delta(C-H)_{ip,ring}$ transitions is 0.95 and 0.94 for the transmission and reflection spectra, respectively. The virtually independent nature of the band ratios is particularly noteworthy for two vibrational modes of the pyrrole ring whose transition dipole moments are *orthogonal* to each other, namely, the in-plane C=C stretch $\nu(C=C)_{ip,ring}$ at ∼1500 cm^{-1} and the symmetric out-of-plane C−H deformation $\omega_s(C-H)_{oop,ring}$ near 720 cm^{-1}; the ratio is 0.35 for the transmission spectrum and 0.27 in the case of the reflection spectrum. Further evidence for the disordered nature of the monolayers is obtained upon examination of the frequency positions of the $\nu_a(CH_2)$ and $\nu_s(CH_2)$ modes in the RAIR spectra, a methodology which allows for a qualitative assessment of the crystalline nature of the methylene chains.[22] The band maxima of the $\nu_a(CH_2)$ and $\nu_s(CH_2)$ modes for **1** on Au are located at 2929 and 2856 cm^{-1}, respectively; values virtually identical to those found in the *liquid* transmis-

(15) (a) Beck, F.; Braun, P.; Oberst, M. *Ber. Bunsen-Ges. Phys. Chem.* **1987**, *91*, 967. (b) Christensen, P. A.; Hamnett, A. *Electrochim. Acta* **1991**, *36*, 1263. (c) Novák, P.; Rasch, B.; Vielstich, W. *J. Electrochem. Soc.* **1991**, *138*, 3300.

(16) (a) Ko, J. M.; Rhee, H. W.; Park, S.-M.; Kim, C. Y. *J. Electrochem. Soc.* **1990**, *137*, 905. (b) Park, D.-S.; Shim, Y.-B.; Park, S.-M. *J. Electrochem. Soc.* **1993**, *140*, 609.

(17) Widrig, C. A.; Chung, C.; Porter, M. D. *J. Electroanal. Chem.* **1991**, *310*, 335.

(18) (a) Assuming 2.1 e/equiv during the oxidation.[17c] The number of electrons involved is dependent on the length of the polymer produced. For example, the value is 2.05 e/equiv for a 10-mer and 2.2 for a 40-mer. Not knowing the length of the polymer/oligomer produced, we have assumed a value of 2.1. (b) Assuming 1 e per 4 equiv for the doping/de-doping process.[18c] (c) Diaz, A. F.; Bargon, J. *Handbook of Conducting Polymers*; Skotheim, T. A., Ed.; Marcel Dekker: New York, 1986; pp 81−115.

(19) (a) Greenler, R. G. *J. Chem. Phys.* **1966**, *44*, 310. (b) Allara, D. L.; Nuzzo, R. G. *Langmuir* **1985**, *1*, 45. (c) Porter, M. D. *Anal. Chem.* **1988**, *60*, 1143A.

(20) (a) Jones, A. R.; Bean, G. P. *The Chemistry of Pyrroles*; Academic Press: New York, 1977. (b) Jones, R. A. *Aust. J. Chem.* **1966**, *19*, 289.

(21) Hostetler, M. J.; Stokes, J. J.; Murray, R. W. *Langmuir* **1996**, *12*, 3604.

(22) (a) Porter, M. D.; Bright, T. B.; Allara, D. L.; Chidsey, C. E. D. *J. Am. Chem. Soc.* **1987**, *109*, 3559. (b) Snyder, R. G.; Schachtschneider, J. H. *Spectrochim. Acta* **1963**, *19*, 85. (c) Schachtschneider, J. H.; Snyder, R. G. *Spectrochim. Acta* **1963**, *19*, 117. (d) Snyder, R. G. *J. Chem. Phys.* **1967**, *47*, 1316. (e) Maroncelli, M.; Qi, S. P.; Strauss, H. L.; Snyder, R. G. *J. Am. Chem. Soc.* **1982**, *104*, 6237.

Table 1. Infrared Band Assignments for 10-(*N*-pyrrolyl)decane-1-thiol

band frequency (cm^{-1})		vibrational mode	
monolayer on planar Au	neat liquid	assignment	direction of transition dipole
signal too small[a]	3100	$\nu(C-H)_{ring}$	∥ to ring
2929	2927	$\nu_a(CH_2)$	⊥ to alkane chain
2856	2855	$\nu_s(CH_2)$	⊥ to alkane chain
N/O[b]	2555	$\nu(S-H)$	
N/O	1669	$\nu(C{=}C)_{ip,ring}$ or $\delta_{ip,ring}$	∥ to ring
1502	1501	$\nu(C{=}C)_{ip,ring}$	∥ to ring
1467	1465	$\delta(CH_2)$	⊥ to alkane chain
1442	1440	$\delta_D(CH_2)$	⊥ to alkane chain
1412	1413	δ_S	⊥ to alkane chain
1372	1371	??	
1356	1358	W_E ?	
1285	1282	$\nu(C-N)_{aliphatic}$	∥ to ring
1089	1089	$\delta(C-H)_{ip,ring}$	∥ to ring
1065	1065	$\delta(C-H)_{ip,ring}$	∥ to ring
969	968	$\omega(C-H)_{oop,ring,a}$	⊥ to ring
N/O	816	??	
722	721	$\omega(C-H)_{oop,ring,s}$	⊥ to ring
N/O	650	??	
616	617	$\omega(C-H)_{oop,ring}?/\delta(C-H)_{ip,ring?}$	

[a] Although there appear to be bands in this region, the signal-to-noise ratio is too small to make band assignments. [b] N/O denotes not observed.

Scheme 2

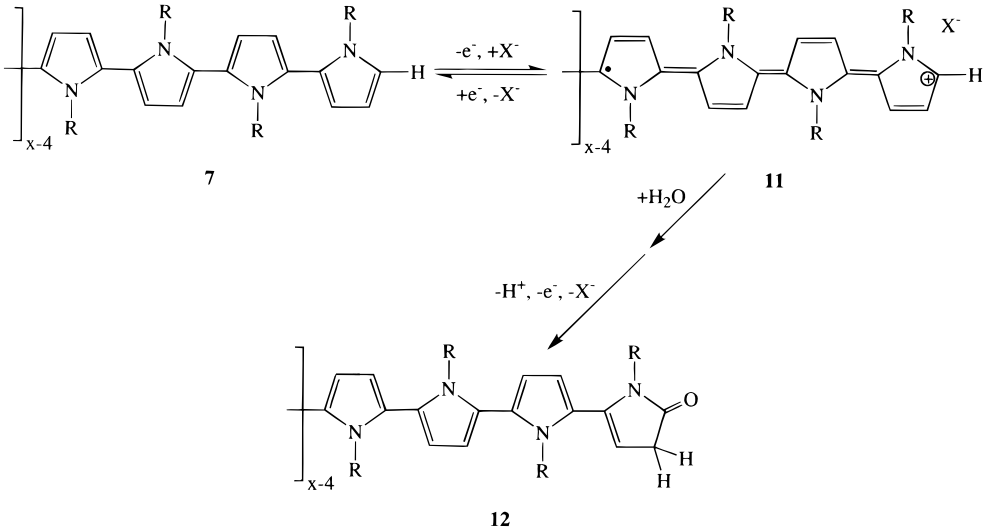

sion spectrum of **1** (2927 and 2855 cm^{-1}). Similar results were observed for **2** and **3** and when assembly times ranging 2 h to 2 days were used. Thus, the infrared spectroscopic data indicates that the structure of the *ω*-(*N*-pyrrolyl)alkanethiol monolayers on Au is such that the pyrrole rings have no particular preferred orientation and the crystallinity of the alkane chain spacer units is very low.

Electrochemically Oxidized *ω*-(*N*-Pyrrolyl)alkanethiol Monolayers. Voltammetry indicative of surface-confined oligomeric or polymeric *N*-alkylpyrroles is observed after treating **1**/Au surfaces as in Figure 1A. Both the shape and potential (E_{poly}) of the surface-confined waves centered at ∼+0.60 V in Figure 1B are characteristic of the electrochemical processes associated with the doping and de-doping of poly(*N*-alkylpyrrole) films formed by electrochemical oxidation of *N*-alkylpyrroles in dry organic electrolytes, Scheme 2.[13] When water or pyridine is present (>∼0.1%) in the Bu_4NClO_4/PC electrolyte, potential excursions to +1.4 V do not lead to observation of the surface waves at +0.60 V, a result characteristic of nucleophilic attack on the pyrrole radical cation.[4a,23,24] Simple *n*-alkanethiol monolayers that have experienced potential excursions such as that in Figure 1A do not exhibit any voltammetric features in this potential region. As expected for an immobilized redox species, the anodic and cathodic peak currents in Figure 1B scale linearly with potential scan rate (over the range of 0.025−0.500 V s^{-1}).[4a,11] The voltammetric response at ∼+0.60 V is stable when the potential scan range limits are 0 and +0.8 V and the electrolyte used does not contain nucleophiles such as water that can lead to degradation of the doped polymer, Scheme 2.[15,16,24] The surface coverage obtained by integration of either the anodic or cathodic waves,[4a,18b] Γ_{poly}, is found to be ∼4 × 10^{-10} mol cm^{-2}, when the background shown by the dotted line in Figure 1B is used, and is independent of the alkane spacer length. The observation that the surface density of the

(23) Morse, N. J.; Rosseinsky, D. R.; Mortimer, R. J.; Walton, D. J. *J. Electroanal. Chem.* **1988**, *255*, 119.

(24) (a) Lei, J.; Cai, Z.; Martin, C. R. *Synth. Met.* **1992**, *46*, 53. (b) Lei, J.; Liang, W.; Martin, C. R. *Synth. Met.* **1992**, *48*, 301. (c) Lei, J.; Martin, C. R. *Synth. Met.* **1992**, *48*, 331. (d) Liang, W.; Lei, J.; Martin, C. R. *Synth. Met.* **1992**, *52*, 227.

monomer, Γ_{ox}, is essentially equal to that obtained from the polymer or oligomer doping/de-doping waves, Γ_{poly}, indicates that conversion of *N*-alkylpyrrole monomer in the monolayer to polymeric/oligomeric material is quite efficient under the conditions used here.

To provide additional evidence that electrochemical oxidation of **1**−**3** on Au results in formation of oligo- or poly(*N*-alkylpyrroles) during potential excursions such as those in Figure 1A, ex situ reflection−absorption infrared spectra were obtained as a function of the oxidation potential. Zerbi has shown for a series of well-defined pyrrole oligomers there are certain vibrational modes that are characteristic of the effective conjugation length (number of pyrrole monomer units contained).[25] In particular, there are three infrared-active modes that can be used to obtain a qualitative determination of the number of contiguous monomer units, namely, the $\nu(C{=}C)_{ip,ring}$, $\delta(C-H)_{ip,ring}$, and $\omega_s(C-H)_{oop,ring}$ modes. In oligo- or poly(pyrroles), each of these modes will be represented by vibrational bands that are associated with the pyrrole backbone and the pyrrole tail groups, leading to observation of two infrared bands for a given mode. The frequency positions for the band maxima of the poly(pyrrole) backbone, known as the *B* modes, are blue shifted with respect to those of the pyrrole tail groups (*T* modes). In addition, as the number of pyrrole repeat units in the chain increases, the intensity of the *B* band in comparison to the *T* band for a given transition ($\nu(C{=}C)_{ip,ring}$, $\delta(C-H)_{ip,ring}$, and $\omega_s(C-H)_{oop,ring}$) will increase. Martin has very successfully used this methodology to correlate the conductivity of variously prepared poly(pyrrole) films to the ratio of the *B* and *T* bands for the $\delta(C-H)_{ip,ing}$ transition.[24] Thus, inspection of the RAIR spectra of **1**−**3** as a function of the oxidation potential should allow for a qualitative assessment of the number of monomer repeat units in the oligomeric/polymeric products formed during potential scans such as that of Figure 1A, as long as the orientation of the pyrrole ring is such so as to allow observation of these modes (the transition dipoles of the $\nu(C{=}C)_{ip,ring}$ and $\delta(C-H)_{ip,ing}$ modes are orthogonal to that of the $\omega_s(C-H)_{oop,ring}$ mode). In addition, changes in the orientation of the alkane tether as a result of possible monolayer reorganization will manifest themselves in the form of changes in the intensity of the $\nu_a(CH_2)$ and $\nu_a(CH_2)$ bands. Furthermore, the RAIR spectra will be useful in determining what other reaction products form during the electrolysis of the *ω*-(*N*-pyrrolyl)alkanethiol monolayers, such as carbonyl- or hydroxyl-substituted pyrroles.

Observations consistent with the formation of dimeric *N*-alkylpyrrole species were noted upon inspection of the RAIR spectra of monolayers **1**−**3** on Au that had experienced potential excursions into the foot of the voltammetric wave (for example 0.50 to 0.20 V negative of $E_{p,ox}$ in Figure 1A). Displayed in Figure 4 are the low-energy RAIR spectra of **1**/Au as a function of electrochemical treatment in 0.1 M Bu_4NClO_4/CH_3CN. We report the anodic potential limit used versus the peak anodic potential of **1**/Au. As can be seen, the intensities of *all* of the infrared bands associated with the in-plane and out-of-plane modes have decreased by the same amount as the potential experienced by the pyrrole monolayer was increased, while only a weak intensity, broad band at 800 cm^{-1} grew in. No significant changes in the intensities of the methylene bands were observed in these experiments. This trend is rather interesting−it suggests that the structure of the monolayer is changing to one where the infrared transitions of the pyrrole moieties are "weaker". Lack of a carbonyl band near 1710 cm^{-1} indicates that the activated pyrrole groups are not forming species that could be attributed to reactions with water and/or oxygen.[14] As noted above, XPS measurements do not support electrochemically induced loss of *ω*-(*N*-pyrrolyl)alkanethiol material from the Au substrate. Even if a reorientation of the pyrrole groups as a result of a change in the interfacial potential led to a stable structure that did not involve covalent bonds between pyrrole units, the fact that the transition dipole moments of the in-plane and out-of-plane modes associated with the pyrrole ring are orthogonal to each other would not lead to a decrease in *all* of the infrared bands, some would display increases in intensity while others would decrease. We propose that the observed uniform decreases in the infrared intensities of the ring modes are due to reaction of activated monomer to produce tethered, dimeric *N*-alkylpyrroles whose rings are oriented parallel to the surface of the Au substrate (vide infra). As opposed to pyrrole, we have found that bipyrrole exhibits two infrared bands for the $\omega_s(C-H)_{oop,ring}$ mode at roughly 796 cm^{-1} (the *B* mode for the out-of-plane deformation, referred to as B_ω) and 720 cm^{-1} (T_ω).[26] In addition, the intensity of the $\omega_s(C-H)_{oop,ring}$ band at 720 cm^{-1} in comparison to that of the in-plane modes in the 1500−1000 cm^{-1} range is much smaller when comparing the spectra of bipyrrole and pyrrole. Both of these observations are in agreement with previous reports.[27] Although this trend in intensities for the B_ω and T_ω modes has also been observed for oligomeric pyrroles containing more than two repeat units, the frequency position of the B_ω mode is ∼30−40 cm^{-1} lower than that of bipyrrole.[25a] Thus, there is a unique infrared signature for dimeric pyrroles, and it leads us to assign the band at ∼800 cm^{-1} to the B_ω mode of the α,α dimer of **1** on the Au surface.[28] Similar results have been obtained for **2**/Au surfaces, as noted in Figure 5B. Here the intensity of the band at 798 cm^{-1} is greater than that seen for **1**/Au in Figure 4. We attribute this difference in intensity to the fact that in this

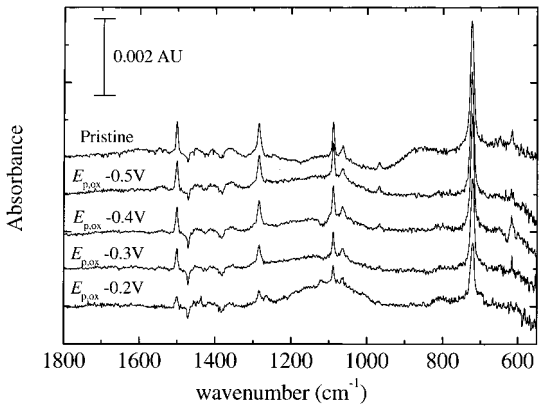

Figure 4. Low-energy region reflection−absorption infrared spectra of **1**/Au as a function of anodic potential limit. In all cases the potential of the samples was scanned to the anodic limit and back to $E_{p,ox}$ −1.15 V (0 V vs Ag QRE) at $\upsilon = 0.10$ V s^{-1}, and then the samples were immersed. The electrolyte was 0.1 M Bu_4NClO_4/propylene carbonate. Each spectrum represents an individual, separate pristine sample that was treated as noted in the figure. A bare Au slide was used as the background.

(25) (a) Zerbi, G.; Veronelli, M.; Martina, S.; Schlüter, A. D.; Wegener, G. *J. Chem. Phys.* **1994**, *100*, 978. (b) Tian, B.; Zerbi, G. *J. Chem. Phys.* **1990**, *92*, 3886. (c) Tian, B.; Zerbi, G. *J. Chem. Phys.* **1990**, *92*, 3892.

(26) Schomburg, K. C.; McCarley, R. L. Unpublished results, 1998.

(27) (a) Street, G. B. *Handbook of Conducting Polymers*; Skotheim, T. A., Ed.; Marcel Dekker: New York, 1986; p. 281. (b) Street, G. B.; Lindsey, S. E.; Nazzal, A. I.; Wynne, K. J. *Mol. Cryst. Liq. Cryst.* **1985**, *118*, 137.

(28) (a) The presence of 3- or 4-substituted *N*-alkylpyrroles as a result of α−*β* coupling reactions is not supported by our IR data. The $\omega_s(C-H)_{oop,ring}$ mode for 3,4-dimethyl-*N*-alkylpyrroles is located at ∼771 cm^{-1} and has an extinction value (230 M^{-1} cm^{-1}) comparable to that of the $\omega_s(C-H)_{oop,ring}$ mode for 2,5-dimethyl-*N*-alkylpyrroles (270 M^{-1} cm^{-1}) at 755 cm^{-1}.[28b] (b) Jones, R. A. *Aust. J. Chem.* **1966**, *19*, 289−96.

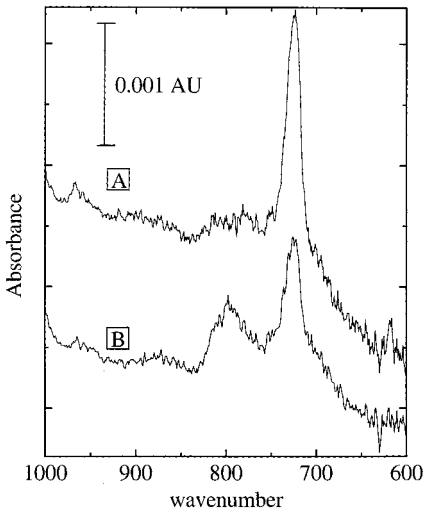

Figure 5. Reflection−absorption infrared spectra of **3**/Au before (A) and after (B) 10 successive voltammetric scans to $E_{p,ox}$ −0.2 V in 0.1 M Bu_4NClO_4/propylene carbonate. A bare Au slide was used as the background.

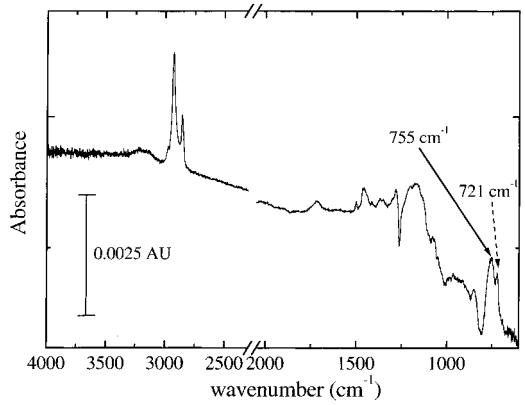

Figure 6. Reflection−absorption infrared spectrum of **1**/Au after a single potential scan to $E_{p,ox}$ −0.1 V and then to $E_{p,ox}$ −1.30 V in 0.1 M Bu_4NClO_4/propylene carbonate at $\upsilon = 0.10$ V s^{-1}. An octadecane-1-thiol-d_{37}/Au slide was used as the background.

case the **2**/Au electrode experienced 10 potential cycles instead of only one, which most likely resulted in the formation of a larger number of the dimeric species.

The use of anodic potential limits that are greater than ∼−0.20 V vs $E_{p,ox}$ for **1**−**3** on Au leads to surfaces which exhibit infrared spectra in the 800−700 cm^{-1} range that are characteristic of oligo(*N*-alkylpyrroles) containing greater than two repeat units. After scanning the potential of **1**/Au between $E_{p,ox}$ −1.15 V and $E_{p,ox}$ −0.10 V and emmersing at $E_{p,ox}$ −1.30 V (−0.15 V vs Ag QRE), the spectrum in Figure 6 was obtained. As can be seen, the intensities of the in-plane modes have decreased to near-baseline values. In addition, the intensity of the $\omega_s(C-H)_{oop,ring}$ band at ∼720 cm^{-1} has decreased by 60% and a new band centered near 755 cm^{-1} is apparent. The latter observation is consistent with the presence of polymeric/oligomeric *N*-alkylpyrroles (B_ω band).[25a] Replicates of this experiment and similar experiments with **2** and **3** yielded values of 755−766 cm^{-1} for the frequency maximum of the B_ω band. When anodic potentials greater than $E_{p,ox}$ but less than $E_{p,ox}$ +0.3 V were used, it was observed that the intensities of the in-plane ring modes dropped to baseline levels, the intensity of the T_ω mode at ∼720 cm^{-1} decreased to <2% of its original value, and once again the B_ω mode became prominent (vide infra). During these experiments, the intensities and frequencies of the $\nu_a(CH_2)$, $\nu_s(CH_2)$, and the methylene deformation bands for the alkane tether remained relatively unchanged (within experimental error), indicating that there neither was any loss of the alkanethiol moiety from the surface nor any large changes in the orientation of the alkane tether. As we outline in more detail later in this paper, it appears that the pyrrole rings have formed an oligomeric/polymeric structure which is oriented such that the in-plane infrared transition dipole moments are parallel or near parallel to the surface, thus rendering their detection extraordinarily difficult with RAIRS. However, in such a scenario the out-of-plane ring modes (B_ω and T_ω modes) should be detectable using RAIRS. The salient point is that the infrared and electrochemical data presented thus far indicate that tethered oligomeric/polymeric *N*-alkylpyrroles are produced under the conditions in Figures 1 and 6. We will discuss the evidence for polymer formation further in a few paragraphs, but now turn our attention to the cause of the carbonyl band at ∼1708 cm^{-1}.

As can be noted from inspection of Figure 6 between 1700 and 1710 cm^{-1}, there is evidence for formation of a small amount of carbonyl-containing material in the pyrrole monolayers upon electrochemical treatment. Even the most favorable inert atmosphere (drybox) and electrolyte (freshly prepared, ∼0.005% H_2O) conditions led to formation of a small intensity carbonyl band during electrochemical oxidation of the *ω*-(*N*-pyrrolyl)alkanethiol monolayers when potentials greater than $E_{p,ox}$ −0.1 V were used. We present this spectroscopic data in order to demonstrate that the oxidized monomeric or polymeric species are susceptible to attack by, what we assume to be, water in the supporting electrolyte media. Previous work with electrochemically prepared poly(pyrroles) indicates that the presence of small quantities of carbonyl-containing material in the poly(pyrroles) has no appreciable affect on the shape of the voltammetric response.[16a,24b,29] The voltammetric response in Figure 1B is unremarkable when compared to that of poly(*N*-alkylpyrroles) found in the literature. However, if the solvent/electrolyte is not carefully dried and anodic potential limits greater than $E_{p,ox}$ are used during the initial oxidation of the monolayer, we have only observed an increase in the double-layer charging current in the potential range (E_{poly}) where the poly(*N*-alkylpyrrole) charging/discharging waves would be expected—a featureless voltammogram is obtained.[4a] Similar observations have been noted when mixed monolayers of **3** and *n*-hexanethiol that contain large amounts of *n*-hexanethiol were investigated in dry electrolyte media (<0.005% H_2O);[4e] under such high-dilution conditions, the pyrrole groups are evidently isolated such that nucleophilic deactivation of the radical cations occurs instead of coupling of activated pyrrole groups. The results for the case at hand point to either deactivation of the monomer cation radical, thus precluding formation of polymer or possible over-oxidation of polymer formed during the voltammetric scan.[15,16,29] Both scenarios would lead to products that do not exhibit a voltammetric response in the potential range where one should observe electrochemistry characteristic of poly(*N*-alkylpyrroles).

We propose that the species formed during the electrochemical oxidation of **1**−**3** on Au in dry electrolyte (<0.005% H_2O), which gives rise to the small carbonyl band between 1700 and 1710 cm^{-1}, is a succinimide. A representative RAIR spectrum of **2**/Au before and after electrochemical over-oxidization[30] ($E_{p,ox}$

(29) Hyodo, K.; MacDiarmid, A. G. *Synth. Met.* **1985**, *11*, 167.

(30) To increase the amount of carbonyl material on the surface for this experiment, we have used a high potential limit. We have found that the amount of carbonyl-containing material increases with increased anodic potential limit and increasing time that the solvent bottle has been open in the drybox. We have not attempted to measure the change in water content in the solvents.

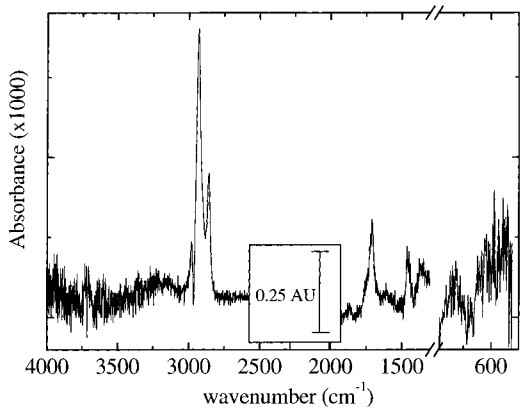

Figure 7. Reflection−absorption infrared spectrum of **2**/Au after a single excursion to $E_{p,ox}$ +0.5 V and then to $E_{p,ox}$ −1.15 V in 0.1 M Bu_4NClO_4/propylene carbonate at $\upsilon = 0.10$ V s^{-1}. An octadecane-thiol-d_{37}/Au slide was used as the background. The region near 1200 cm^{-1} exhibits spectral behavior indicative of sample/reference damage (absorptions due to Si−O stretches) and is not displayed.

+0.50 V) is displayed in Figure 7. A strong absorption at 1708 cm^{-1} characteristic of carbonyl functionalities and the bands corresponding to the methylene modes at 2930, 2857, and 1465 cm^{-1} are present, but the bands associated with the aromatic ring modes no longer display measurable absorptions. In addition, there is a ∼10% decrease in the intensity of the $\nu_a(CH_2)$ and $\nu_s(CH_2)$ bands, pointing to a possible decrease in the tilt angle of the alkane chain. Several authors have discussed the various products that form during the autoxidation of *N*-methylpyrrole (Scheme 1) or when poly(*N*-methylpyrrole)/poly(pyrrole) is electrochemically oxidized or over-oxidized in the presence of water (Scheme 2); the products include pyrrolinones/hydroxypyrrole tautomers (*N*-methyl-3-pyrrolin-2-one, 3-pyrrolin-2-one-terminated polymers), maleimides (*N*-methylmaleimide), and succinimides (*N*-methylsuccinimide).[14a−16,29] The following pieces of information support the conclusion that the product formed is a tethered *N*-alkylsuccinimide: (1) the carbonyl stretch ν(C═O) for *N*-methylsuccinimide is centered near 1701 cm^{-1}, (2) the carbonyl band is found at ∼1675 cm^{-1} for both *N*-methyl-3-pyrrolin-2-one and 4-methoxy-3-pyrrolin-2-one, while the peak frequency for this mode is located at 1639 cm^{-1} for *N*-methylmaleimide, and (3) 4-methoxy-3-pyrrolin-2-one is known to have a strong $\omega_s(C-H)_{oop,ring}$ mode at 730 cm^{-1}, but no bands are observed in the frequency range of 800−700 cm^{-1} in Figure 7 or in the spectrum of *N*-methylsuccinimide. In addition, our data do not indicate the possibility of a hydroxypyrrole or poly(hydroxypyrrole) surface,[24c] for there is no ν(O−H) band present near 3580 cm^{-1} in Figure 7. Thus, we conclude that the tethered pyrrole functionalities are converted to succinimides during the electrochemical over-oxidation of **1**−**3** on Au. The use of carefully dried electrolytes and proper anodic oxidation potentials is necessary in order to successfully obtain spectra such as those in Figures 4−6 and voltammograms such as that in Figure 1B. These data are strong evidence for formation of a polymeric pyrrole layer.

The proposed structure of the pyrrole monolayers upon electrochemical oxidation in dry electrolyte media is one which has tethered oligomeric/polymeric pyrroles of various monomer repeat units with the pyrrole rings oriented parallel to the surface, Figure 8B.[4a] On the basis of the data presented thus far, a general scheme for the oligomerization/polymerization can be proposed. A highly isotropic initial pyrrole monolayer structure, Figure 8A, should provide sufficient pyrrole group mobility for successful α,α coupling of the radical cations produced during

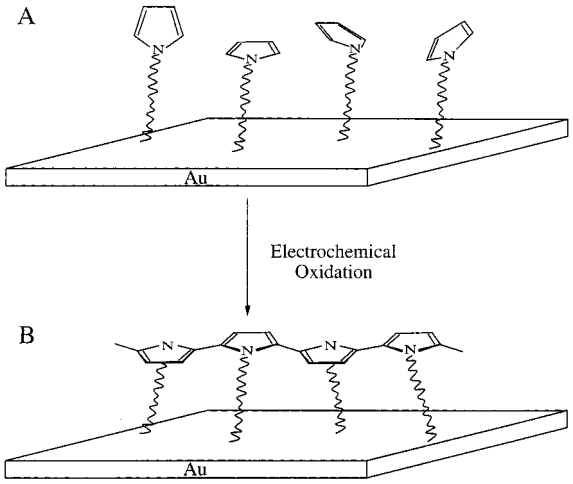

Figure 8. Schematic representation of the pyrrole monolayers before (A) and after (B) electrochemical oxidation.

electrochemical oxidation. Presumably, the coupling reactions will continue until the growing oligomer/polymer chains reach a given effective conjugation length,[31] a length that is dictated by the ability of the activated pyrrole groups and growing polymer chains to move toward each so that coupling can occur[31] or by known termination reactions, such as nucleophilic attack of water on the growing pyrrole polymer chains to yield a (pyrrolin-2-one)-terminated polymer chain (**12**).[18c] Assuming a polymer structure such as that in Figure 8B, only those vibrational modes with sufficiently strong transition dipole moments oriented perpendicular to the surface will be observed in the RAIR spectrum. It has been shown that the directions of the transition dipole moments of the vibrational modes of the pyrrole ring do not change upon polymerization.[25,33] Thus, for the proposed monolayer structure in Figure 8, we would expect to observe only the B_ω and T_ω modes of the expected α,α-connected polymer/oligomer at ∼760 cm^{-1} [28,34] but all the transitions associated with the alkane tether. In addition, even though conditions have been adopted so as to minimize its formation, one would expect to observe a small amount of species on the surface resulting from nucleophilic attack of water on the monomer radical, namely, carbonyl-containing species. Our infrared data support such a structure.

The previously mentioned infrared data on 3−20 monomer repeat oligomeric pyrroles[25a] can be used to approximate[35a] the number of repeat units or effective conjugation length in the tethered poly(*N*-alkylpyrroles). For example, from the ratio of

(31) This is defined as the number of defect-free contiguous monomer units in the chain.[24,25]

(32) Due to the isotropic nature of the pyrrole monolayers, the ability of the activated pyrrole groups to move about should not be greatly affected by the length of the alkane tether.

(33) Kostic, R.; Rakovic, D.; Stepayan, S. A.; Davidova, I. E.; Gribov, L. A. *J. Chem. Phys.* **1995**, *102*, 3104.

(34) The extinction coefficient for the $\omega_a(C-H)_{oop,ring}$ mode for 2,5-dimethyl-*N*-alkylpyrroles is found to be 10 M^{-1} cm^{-1} in comparison to 80 M^{-1} cm^{-1} for unsubstituted *N*-alkylpyrroles and is found to decrease with increasing electron-donating capability of ring substituents.[19,27b] We feel that the intensity of the $\omega_a(C-H)_{oop,ring}$ mode for the polymers made here would be such that it would go undetected.

(35) (a) We must stress that this method is an approximation, for as Zerbi states, "the intensity of these bands should not be assumed to be linear with the number of units since the delocalization of π electrons which takes place along the chain can change the intrinsic absorption coefficient of each oligomer." Thus, we have based our assignment of repeat lengths on the closest value of the observed intensity ratio (B_ω mode to the T_ω mode) to that of the specific oligomers reported in Zerbi's work.[25a] (b) Due to the lack of any infrared data on pyrrole oligomers containing more than 20 monomer units, this number is possibly too small.

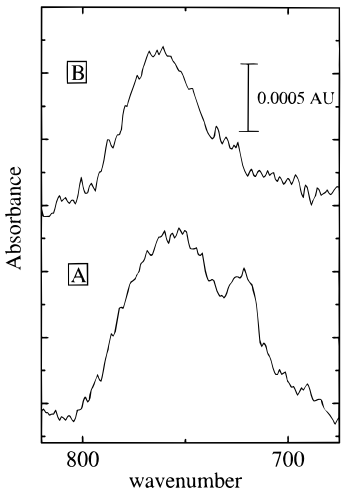

Figure 9. Reflection−absorption infrared spectra of **1**/Au after a single potential excursion to $E_{p,ox}$ −0.1 V (A) and $E_{p,ox}$ (B) in 0.1 M Bu_4NClO_4/propylene carbonate at $\upsilon = 0.10$ V s^{-1}. An octadecane-1-thiol-d_{37}/Au slide was used as the background in A, and a bare Au slide was used as the background in B.

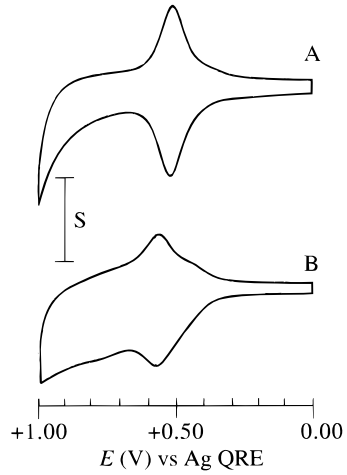

Figure 10. Cyclic voltammograms of **1**/Au surfaces that have been exposed to a 0.25 mM ethanolic solution of $(C_5H_5)Fe(C_5H_4(CH_2)_8SH)$ for 135 min. (A) The **1**/Au electrode was transferred to the 0.25 mM solution of $(C_5H_5)Fe(C_5H_4(CH_2)_8SH)$ without electrochemical treatment. (B) The **1**/Au electrode was transferred to the 0.25 mM solution of $(C_5H_5)Fe(C_5H_4(CH_2)_8SH)$ after a single potential excursion to $E_{p,ox}$ (+1.15 V vs Ag QRE) in 0.1 M Bu_4NClO_4/propylene carbonate. Conditions for A and B: $\upsilon = 0.10$ V s^{-1}, 0.1 M Bu_4NClO_4/propylene carbonate and $S = 7.7 \times 10^{-6}$ A cm^{-2}. The slight shift in the potential of the ferrocene wave upon comparison of A to B is a result of the normal variations observed when using an Ag QRE.

the integrated band intensity of the B_ω mode to the T_ω mode in Figure 9A for a **1**/Au sample scanned to $E_{p,ox}$ −0.1 V, we estimate the average number of pyrrole units in the chain to be approximately 7. Similarly, from the data in Figure 9B where the monolayer experienced an anodic potential of $E_{p,ox}$, the number of monomer repeats is estimated to be roughly 20, but could be much higher.[35b] As expected, the use of a higher anodic potential limit—thus resulting in a higher amount of charge passed for production of more $\mathbf{1}^+$ and the cation of the oligomers of **1**—for the electrochemical polymerization of the pyrrole monolayer leads to larger effective conjugation lengths. It must be stressed that these are average values for the number of pyrrole groups in the chain—there is most likely a distribution in the number of pyrrole units in the backbone. *The important finding from the data presented here is that tethered poly(N-alkylpyrroles) with various monomer repeat lengths can be made by electrochemically oxidizing **1**−**3**/Au surfaces in dry organic electrolytes.*

As a final comment regarding the possibility of having pyrrolin-2-ones as the end groups on the tethered poly(*N*-alkylpyrroles) **12**, we turn to a discussion of the RAIR spectrum in Figure 6. It is well-known that the band for the carbonyl stretch of pyrrolin-2-ones is centered near 1670 cm^{-1}, while the band associated with the C−H out-of-plane deformation mode for the ring is located near 730 cm^{-1}.[14,29] Upon close inspection of Figure 6, no absorptions are noted within the immediate vicinity of these two frequencies. On the basis of our proposed structure of the tethered poly(*N*-alkylpyrroles) shown in Figure 8B, the ν(C═O) transition is not expected to be observed in the RAIR spectrum. However, that of the ω_s-$(C-H)_{oop,ring}$ mode should be, if indeed there is a reasonable population of these chain-end defects. We cannot say with certainty that there is none of the pyrrolin-2-one functionality on the surface, for its $\omega_s(C-H)_{oop,ring}$ band could possibly be obscured by the B_ω and T_ω modes of the poly(*N*-alkylpyrroles). Thus, if the polymer chains are terminated by the pyrrolin-2-one functionalities, the amount present must be extremely small.

In summary, the electrochemical and infrared spectroscopic evidence presented here strongly support the production of polymerized ω-(*N*-pyrrolyl)alkanethiol monolayers on Au surfaces when proper electrochemical conditions are used. Furthermore, the effective conjugation length or degree of polymerization of the tethered pyrroles is dependent on the potential used to polymerize the surface-confined monomers on the electrode surface. Future work will focus on correlation of mass spectrometrically determined polymer molecular weights[36] with those values of monomer repeat length obtained from infrared measurements, as a function of electrochemical treatment. In addition, future investigations will include RAIRS and XPS studies of the doping/de-doping process associated with the tethered poly(*N*-alkylpyrrole) monolayers so as to assess their possible use in nanoscopic electronic devices.

Polymerized Monolayer Stability toward Thiol Exchange. The stability that the polymerized pyrrole monolayers offer toward monolayer loss in solution as a result of displacement by donor solvents can be readily assessed through the use of thiol exchange experiments.[37] Exposure of a given pyrrole monolayer to a solution of the redox-labeled alkanethiol, $(C_5H_5)Fe(C_5H_4(CH_2)_8SH)$,[38] can be used to probe the integrity of the pyrrole monolayer. By monitoring the voltammetric response in the potential range where the ferrocene group is expected to undergo electron transfer, one can obtain a qualitative idea of what fraction of the pyrrole monolayer is displaced during the exchange experiment. Shown in Figure 10 are the cyclic voltammograms of **1**/Au and poly-**1**/Au after exposure to a 1 mM solution of $(C_5H_5)Fe(C_5H_4(CH_2)_8SH)$ in ethanol for 135 min. The redox response of the ferrocenyloctanethiol overlaps with that of the tethered poly(*N*-alkylpyrroles), but its shape is vastly different, allowing for qualitative assessment of pyrrole monolayer loss during the exposure. After 135 min of exposure to the ferrocenyloctanethiol, the voltammetry of poly-

(36) (a) Li, Y.; Huang, J.; McIver, R. T. Jr.; Hemminger, J. C. *J. Am. Chem. Soc.* **1992**, *114*, 2428. (b) McCarley, T. D.; McCarley, R. L. *Anal. Chem.* **1997**, *69*, 130.

(37) (a) Chidsey, C. E. D.; Bertozzi, C. R.; Putvinski, T. M.; Mujsce, A. M. *J. Am. Chem. Soc.* **1990**, *112*, 4301. (b) Collard, D. M.; Fox, M. A. *Langmuir* **1991**, *7*, 1193. (c) Rowe, G. K.; Creager, S. E. *Langmuir* **1991**, *7*, 2307. (d) Groat, K. A.; Creager, S. E. *Langmuir* **1993**, *9*, 3668.

(38) (a) A kind gift from Prof. L. S. Curtin prepared as previously described.[38b] (b) Curtin, L. S.; Peck, S. R.; Tender, L. M.; Murray, R. W.; Rowe, G. K.; Creager, S. E. *Anal. Chem.* **1993**, *65*, 386.

1/Au indicates that only ~25% of the monolayer has exchanged, while for the same time period, it can be seen that effectively all of the untreated pyrrole monolayer has been displaced by the $(C_5H_5)Fe(C_5H_4(CH_2)_8SH)$. Similar results have been obtained for **3**/Au. After a 1 day exposure to the ferrocenyloctanethiol, polymerized **1**/Au and **3**/Au exhibit voltammetry that points to complete exchange by the ferrocenyloctanethiol. These results demonstrate that the electrochemical polymerization of the pyrrole layers indeed increases the stability of the monolayer toward an extremely aggressive competing adsorbate and indicate that stabilization strategies based on polymerizable alkanethiol monolayers[4] should be beneficial in the construction of stabilized molecular assemblies.

Summary

Polymerizable self-assembled monolayers based on pyrrole monomers have been shown to undergo coupling reactions to form oligomeric/polymeric surfaces as demonstrated by electrochemical and infrared analysis. These polymerized monolayers can be formed from monolayers which have alkane tethers of various lengths, indicating that the tether group and the pyrrole group in the original monolayer are quite isotropic (disordered) so as to allow for great monomer group motion; infrared spectra of the pristine monolayers support such a hypothesis. The most striking result from the study at hand is that the polymerized pyrrole monolayers are quite stable with respect to exhange by a solution-phase alkanethiol. This result compares favorably with those from the Crooks[4d] and Schlenoff[4f] groups, where it has been shown that polymerized organothiol monolayers are quite difficult to remove by either electrochemical or laser-desorption methods. Collectively, the work that has been accomplished to date with polymerizable organothiol monolayers would seem to indicate that such layers, once polymerized, will be excellent platforms onto which robust sensors and devices may be fabricated. The challenge now is the further development of polymerizable monolayers that (1) can be readily modified using traditional synthetic approaches so as to allow for "building on top of" the polymerized platform (as has been done by the Crooks group with ω-terminated diacetylene monolayers), (2) can be polymerized using a variety of chemistries (thus requiring a greater selection of monomer substituents) so as to afford layers that can be processed using methods acceptable to the microfabrication industry, and (3) will be amenable to nontraditional micro- and nanodevice fabrication protocols such as those associated with the scanning probe microscope.

Experimental Section

Chemicals. Bu_4NClO_4 was synthesized and purified as described in the literature.[39] Pyrrole [109-97-7] (Aldrich, 98%), 1,10-dibromodecane [4101-68-2] (Aldrich, 97%), 1,7-dibromoheptane [4549-31-9] (Aldrich, 97%), 1,6-dibromohexane [629-03-8] (Aldrich, 98%), thiourea [62-56-6] (Aldrich, 99%), semiconductor grade potassium hydroxide and sodium hydroxide (Aldrich), potassium ferricyanide [13746-66-2] (Aldrich, 99+%), and 1-bromoooctadecane-d_{37} [112-89-0] (CDN Isotopes, 99.6 atom % D) were used as received. Octadecane-1-thiol-d_{37} was synthesized from the bromide according to the literature.[4h,40] Acetonitrile [75-05-8] (Aldrich, Sure-Seal, ≤0.005% H_2O) and propylene carbonate [108-32-7] (Aldrich, Sure-Seal, <0.005% H_2O) were used without further purification and were opened and stored in the drybox. Distilled water was passed through a Barnstead reverse osmosis filter followed by a Nanopure water system to yield water with a resistivity of 18 MΩ cm. All other chemicals were reagent grade or better.

Synthesis of ω-(*N*-Pyrrolyl)alkanethiols. Compounds **1**−**3** were synthesized from the corresponding ω-(*N*-pyrrolyl)-1-bromoalkanes[40] by conversion to the thiouronium salt followed by base hydrolysis.[4h,41] The purity of the three ω-(*N*-pyrrolyl)alkanethiols was greater than 99.2% as noted by gas chromatography/mass spectrometry. MS {*m*/*z*, rel intensity, EI (70 eV)} for **3**: 183 and 185 (M^+, 23.2 and 1.2 (A + 2)), 150 (M^+ − SH, 61.1), 81 ($C_4H_4NCH_3^+$, 100), 80 ($C_4H_4NCH_2^+$, 77.3), 68 ($C_4H_4NH^+$, 19.2), 67 ($C_4H_4N^+$, 16.3). For **2**: 197 and 199 (M^+, 20 and 1 (A + 2)), 164 (M^+ − SH, 35.3), 81 ($C_4H_4NCH_3^+$, 100), 80 ($C_4H_4NCH_2^+$, 54.4), 68 ($C_4H_4NH^+$, 12.9), 67 ($C_4H_4N^+$, 12.1). For **1**: 239 and 241 (M^+, 19 and 1.1 (A+2)), 206 (M^+ − SH, 21), 81 ($C_4H_4NCH_3^+$, 100), 80 ($C_4H_4NCH_2^+$, 36.8), 68 ($C_4H_4NH^+$, 7.9), 67 ($C_4H_4N^+$, 6.8).

Monolayer Formation. Au substrates for infrared studies were prepared as previously described[4h] using evaporative metal deposition. All monolayer formation was carried out in an inert atmosphere drybox (Vacuum Atmospheres). Upon removal from the evaporator, the Au substrates were immediately transferred to the drybox under Ar-purged absolute ethanol in sealed vials. The Au substrates were rinsed with pure ethanol and then incubated in ~1mM solutions of **1**−**3** in absolute ethanol for a minimum of 2 h. After assembly, the samples were rinsed with copious amounts of ethanol and allowed to dry in the drybox.

Electrochemical Measurements. Electrochemistry was performed in normal three-electrode mode with a PAR 273A potentiostat/galvanostat and conventional glass electrochemical cells inside the controlled atmosphere box. Potentials were recorded against an Ag/Ag^+ quasi-reference electrode (QRE). In addition to the Au film electrodes, Au wires sealed in glass were used. The wire electrodes were mechanically polished using various grit diamond pastes, followed by 0.05 μm alumina, and then electropolished in 1 M $HClO_4$ immediately before further use. Surface roughness of the wire electrodes was assessed as previously described,[4a] with the values being near 2.

Infrared Spectroscopy. All infrared spectra were obtained with a Nicolet 740 FTIR system with wide and narrow band detectors having low energy cutoff values of 550 and 780 cm^{-1}, respectively. A custom-made poly(ethylene) shroud continuously purged with house nitrogen (liquid nitrogen boil-off) protected the analyzing chamber from water and CO_2 contamination. The optical bench was purged with house nitrogen passed through a homemade water and CO_2 scrubbing system. Reflection spectra were collected using a versatile reflection accessory with retromirror attachment (VRA-RMA, Harrick Scientific) using incidence angles of 86° with respect to the substrate normal. Spectra were typically recorded using 1024 co-added scans at 2 cm^{-1} resolution with Happ-Genzel apodization. Purge correction to remove residual water vapor bands from the infrared RA spectra was typically used. Baseline correction of spectra was performed using the Nicolet SX software. The purge time before spectral collection was roughly 20 min. Both bare Au and octadecane-1-thiol-d_{37}/Au were used as background references.

XPS Analysis. X-ray photoelectron analysis was performed on a Kratos XPS spectrometer employing a monochromatic Al Kα source at 1486.6 eV. The anode voltage was 12 kV, and the anode current was ~20 mA.

Acknowledgment. This research was supported by the National Science Foundation (CHE-9529770) and the Louisiana Education Quality Support Fund (LEQSF(1993-96)-RD-A-09). We thank Professor I. Fritsch at the University of Arkansas for obtaining the XPS data shown in Figure 2.

JA981677D

(39) Sawyer, D. T.; Roberts, J. L. *Experimental Electrochemistry For Chemists*; Wiley: New York, 1984; p 212.

(40) Willicut, R. J.; McCarley, R. L. *Langmuir* **1995**, *11*, 296.

(41) *Chemistry of the Thiol Group*; Patai, S., Ed.; Wiley: New York, 1974.